Journal of Alloys and Compounds 509 (2011) 9425–9427

Contents lists available at ScienceDirect

Journal of Alloys and Compounds

journal homepage: www.elsevier.com/locate/jallcom

Growth and characteristics of Zn–Se–S thin layers by dip method

P.A. Chate [a,*], D.J. Sathe [b], P.P. Hankare [c]

[a] Dept. of Chemistry, J.S.M. College, Alibag 402 201, India
[b] Dept. of Chemistry, KITs College of Engineering, Kolhapur, Maharashtra, India
[c] Solid State Research Lab, Dept. of Chemistry, Shivaji University, Kolhapur 416 004, India

ARTICLE INFO

Article history:
Received 27 May 2011
Received in revised form 18 June 2011
Accepted 23 June 2011
Available online 30 June 2011

Keywords:
Nanostructures
Semiconductors
Thin films
Chemical synthesis

ABSTRACT

Zn–Se–S composite thin films of mixed cubic and hexagonal phases of ZnSe and ZnS are synthesized by dip process at room temperature. Polycrystalline nature of the films was observed from XRD. Optical band gap of Zn–Se–S thin film was found to be in between individual band gaps of ZnSe and ZnS. The electrical conductivity was found to be in the range of 10^{-5}–10^{-2} $(\Omega\,cm)^{-1}$. Due to above properties, these films find applications as a buffer layer in solar cells.

1. Introduction

Recent investigations have evoked considerable interest in sulphide and selenide thin films due to their vast possible applications [1,2]. Zinc sulphide and zinc selenide belong to the II–VI family of semiconducting materials receiving ever-increasing attention in both bulk and thin film forms [3,4]. ZnS can be used for the fabrication of optoelectronic devices such as blue-light emitting diodes, electroluminescent devices, electro-optic modular, optical coating, n-indo layers for thin film heterojuncion solar cells, photo conductor, and photo voltaic devices [5–8]. It is used in beam splitting and band pass filters over the region between 400 and 1000 nm [9–11]. Because of its high refractive index (2.35), and a dielectric filter, it is used as reflector in the visible region [12]. Structural and fluorescence studies on chemically deposited ZnS thin film have been made by Cruz-Vazquez et al. [13]. Optical reflectance spectra of ZnS thin film are reported by Kumar et al. [14]. Oztas et al. studied effect of annealing on morphology and optical properties of ZnS thin films [15]. ZnSe is one of the important materials as buffer layer in copper indium selenide based solar cells because of better conformity of lattice parameter and non-toxicity. Also, it has potential applications in red, blue and green light emitting diodes, photovoltaic, laser screens, thin-film transistor, and photoelectrochemical cells [16–18]. Being a direct band gap, photonic material, ZnSe is capable of emitting light in the blue-green region with a wavelength of 460 nm [19]. Ternary alloys like $Zn_{1-x}Cd_xSe$, $ZnSe_{1-y}S_y$ are best materials for optoelectronic device technology in the blue region of visible spectrum [17,20]. Optical and electrical studies on chemically deposited ZnSe thin film have been made by Kale and Lokhande [21]. The Raman spectra and photoluminescence studies have been reported by Jan et al. [22]. Optical selection rule is reported by Mitusumori et al. [23]. Bouroushian et al. studied photoelectrochemical properties of ZnSe thin film in sulphide and polysulphide and ferro-ferricyanide redox system [24]. In this report, emphasis was made to synthesis composite Zn–Se–S composite thin films and characterized for structural, optical and electrical properties.

2. Experimental details

All the chemicals used for the deposition were of analytical grade. It includes zinc sulphate heptahydrate, tartaric acid, liquor ammonia, hydrazine hydrate and thiourea, sodium sulphite and selenium. All the solutions were prepared in double distilled water. Sodium selenosulphate was prepared by following the method reported earlier [25]. In actual experimentation, 10 mL (0.2 M) zinc sulphate heptahydrate solution was taken in 100 mL beaker. 2.5 mL (1 M) tartaric acid, 25 mL (2.8 M) ammonia, 25 mL (2%) hydrazine hydrate and 5 mL (0.2 M) thiourea, 5 mL (0.2 M) sodium selenosulphate were added into the same reaction bath. The pH of the reactive mixture is 11.54. The temperature of the bath was maintained at 278 K using ice bath. Individual solutions were cooled at 278 K and mixed to avoid precipitation. The solution was stirred vigorously before dipping non-conducting glass substrates. The substrate was kept vertically slightly tilted in the reactive bath. The temperature of the bath was then allowed to increases up to 303 K very slowly. After 7 h, the slides were removed and washed several times with double distilled water. The film was dried naturally and preserved in dark desiccators over anhydrous $CaCl_2$.

* Corresponding author. Tel.: +91 0231 2693501.
E-mail addresses: pachate04@rediffmail.com, pachate09@rediffmail.com (P.A. Chate).

0925-8388/$ – see front matter © 2011 Elsevier B.V. All rights reserved.
doi:10.1016/j.jallcom.2011.06.101

3. Results and discussion

3.1. Growth mechanism

The release of metal ions by the complexing species is a thermally activated process [26]. In the reaction bath, Zn^{+2} ions are complexed with tartaric acid in the form of water-soluble Zn–tartarate complex and thus control Zn^{+2} concentrations. The dissociation of sodium selenosulphate, thiourea as well as Zn–tartarate complex in alkaline medium takes place. Homogenous system was observed at 278 K. This is due to the fact that metal ions are in a stable complexed state and the ionic product of cation and anions does not exceed solubility product. To get the free cation and anions, the temperature of the reactive bath increases slowly to room temperature. The increase in temperature results in the dissociation of metal complex, sodium selenosulphate and thiourea to obtain Zn^{+2}, Se^{-2}, S^{-2} ions, which combine to obtain a thin film. The kinetic growth of film can be understood from the following:

$$Zn^{+2} + \text{Tartaric acid} \rightarrow [\text{Zn–tartarate}]$$

$$SC(NH_2)_2 + OH^- \rightarrow HS^- + CH_2N_2 + 2H_2O$$

$$HS^- + OH^- \rightarrow S^{-2} + H_2O$$

$$Na_2SeSO_3 + OH^- \rightarrow Na_2SO_4 + HSe^-$$

$$HSe^- + OH^- \rightarrow H_2O + Se^{-2}$$

$$[\text{Zn–tartarate}] + Se^{-2} + S^{-2} \rightarrow \text{Zn–Se–S} + [\text{tartarate}]^{-2}$$

The film formation takes place by recombination of ions on the substrate surface via nucleation followed by growth process. Since the solubility product of ZnSe is lower than that of ZnS [K_{sp} (ZnSe) = 10^{-31} and K_{sp} (ZnS) = $10^{-24.7}$], ZnSe layer acts as a catalyst for a further growth of film. This layer adsorbs more and more Zn^{+2}, S^{-2} and Se^{-2} ions to form ternary Zn–Se–S thin film.

There are several soluble and insoluble species of Zn^{+2} possible in a reaction bath containing OH^-. The pH of reactive mixture is less than 7.5 or greater than 13.7, soluble species such as Zn^{+2} and ZnO^{-2} are present, respectively. If the pH of the bath is in between 7.5 and 13.7, then insoluble $Zn(OH)_2$ may be present [27]. The presence of $Zn(OH)_2$ in the reaction mixture is unavoidable due to aqueous alkaline nature of the bath. The amount of $Zn(OH)_2$ increases with increase in temperature. This results in the inclusion of $Zn(OH)_2$ in the ZnSe film resulting in the formation of $Zn_x(Se,OH)_y$ thin film rather than ZnSe film [28]. An increase in deposition temperature favors the homogenous precipitation rather than the film formation, which causes saturation to occur. Both hydrazine hydrate and ammonia are necessary for the formation of films and hydrazine hydrate might be playing a complexing and/or catalytic role in the film process [29,30], which improves compactness and adherence of the films.

The thickness of the thin film was measured by weight difference method and found to be 0.48 μm.

3.2. X-ray diffraction

X-ray diffraction pattern of Zn–Se–S thin film is shown in Fig. 1. The presence of a large number of peaks indicates that the films are polycrystalline in nature. The chalcogenide of zinc normally shows the duality in their crystal structure. They can be formed with either cubic zinc blend or hexagonal wurtzite type structure [4,31]. At experimental conditions, ZnSe shows cubic structure while ZnS observed in hexagonal phase. No ZnSe hexagonal and ZnS cubic phase as observed. It is interesting to note that thin film shows formation of admixture, independent phase. The spectra for pure ZnSe [JCPDS-1463] and pure ZnS [JCPDS-39-136] were used for identification purpose. The analysis of XRD pattern in terms of *hkl* planes, interplanar distance, crystallite size and microstrain has been done. The most intense reflection observed for thin film was originating from cubic (1 1 1) plane of ZnSe. The high intensity reflection peak observed at d = 3.273 Å (1 1 1). Similarly, (0 0 8) plane of hexagonal ZnS was observed at d = 3.512 Å. The grain dimension was calculated by Debye–Scherer relationship [32]. The average crystallite size was calculated by resolving the intense peak. It was found to be 84.85 nm.

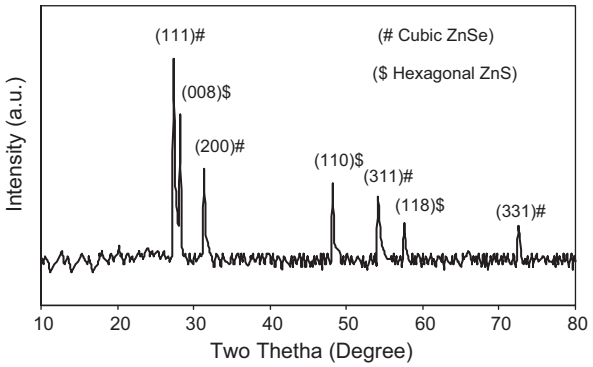

Fig. 1. X-ray diffraction pattern of Zn–Se–S thin film.

3.3. Optical studies

The optical property of deposited thin film was studied at room temperature from absorption measurement in the range of 300–600 nm and is shown in Fig. 2. The absorbance spectrum shows a sharp increase in absorption at wavelength near to absorption edge at the threshold wavelength for onset of absorption, and the energy corresponding to this determines the band gap of the semiconducting material. The Zn–Se–S film shows absorption coefficient (α) 9.7 × 10^3 cm^{-1} near absorption edge. This shows that the deposited semiconducting film is a direct band gap material [33]. For allowed transition $(\alpha)^2$ is plotted against photon energy to give a straight line for direct transition as shown in Fig. 3, from which band gap is found to be 3.19 eV. It falls between the band gap value of ZnSe (2.7 eV) and ZnS film (3.6 eV) [34,35].

3.4. Electrical properties

The conductivity of all samples was measured by using two probe methods, in temperature range of 300–525 K for heat-

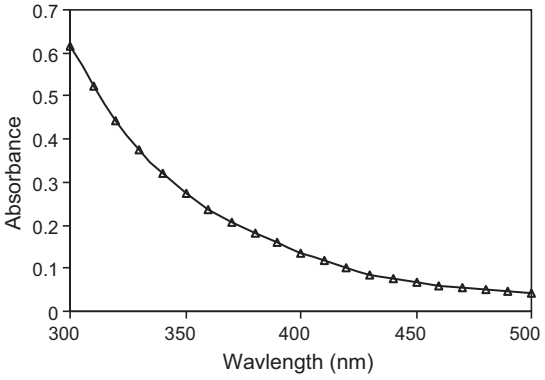

Fig. 2. Absorption spectrum of Zn–Se–S thin film.

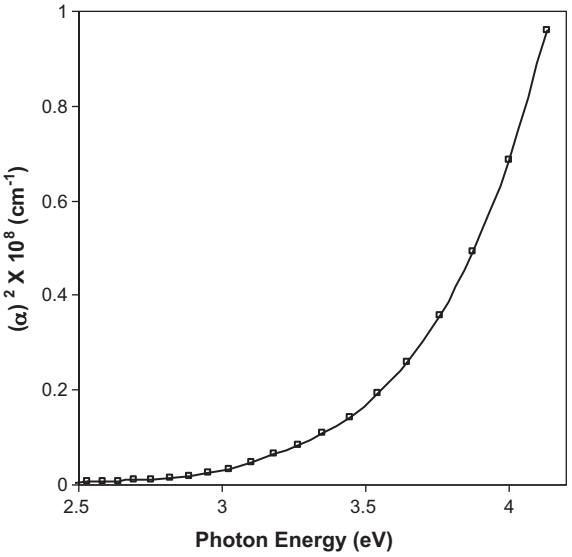

Fig. 3. A plot of $(\alpha)^2$ against Photon energy.

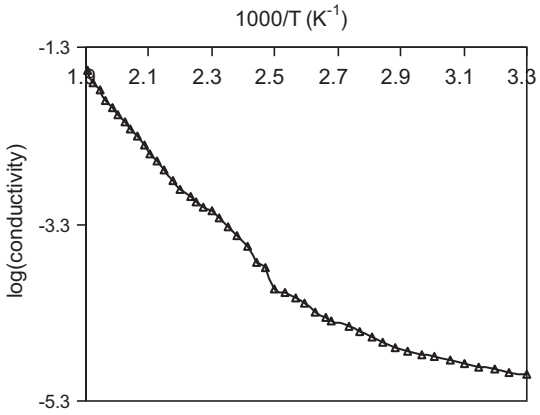

Fig. 4. A plot of log (conductivity) versus absolute temperature.

ing and cooling cycles. The electrical conductivity variation with temperatures during heating and cooling cycles was found to be different and this shows that the 'as-deposited' film undergoes irreversible changes due to annealing out of non-equilibrium defects during first heating. The specific conductance was found to be $1.01 \times 10^{-5}\,(\Omega\,\mathrm{cm})^{-1}$ and $2.74 \times 10^{-2}\,(\Omega\,\mathrm{cm})^{-1}$ at 300 and 525 K, respectively. The conductivity of the samples increases with increase in temperature, showing semiconducting behavior of the films. The plot of log (conductivity) versus 1000/T is shown in Fig. 4. A plot shows that electrical conductivity has two linear regions, the low temperature extrinsic and high temperature intrinsic regions, indicating the presence of two conduction mechanisms. The high temperature region is due to grain boundary scattering limited conduction mechanism, while a low temperature region is due to variable range hopping conduction mechanism. The activation energies have been computed from high and low temperature regions by using Arrehenius equation. It was found to be 0.052 and 0.58 eV at low and high temperature, respectively.

4. Conclusions

Zn–Se–S composite thin films are deposited by chemical method using hydrazine hydrate as a complementary complexing agent. It is obtained by using zinc sulphate, sodium selenosulphate, and thiourea as Zn^{+2}, Se^{-2} and S^{-2} ion sources. Different phases of ZnSe and ZnS were observed from X-ray diffraction. The band gap and electrical conductivity of the film were 3.19 eV and $10^{-5}\,(\Omega\,\mathrm{cm})^{-1}$, respectively.

References

[1] A.U. Ubale, D.K. Kulkarni, Bull. Mater. Sci. 28 (2005) 43.
[2] P.A. Chate, D.J. Sathe, P.P. Hankare, J. Mater. Sci.: Mater. Electron. 22 (2011) 111.
[3] P. Roy, J. Ota, S. Srivastava, Thin Solid Films 515 (2006) 1912.
[4] P.P. Hankare, P.A. Chate, M.R. Asabe, S.D. Delekar, I.S. Mulla, K.M. Gardkar, J. Mater. Sci.: Mater. Electron. 17 (2006) 1055.
[5] S. Yamaga, A. Yoshokawa, H. Kasin, J. Cryst. Growth 86 (1998) 252.
[6] I.C. Ndukwe, Sol. Energy Mater. Sol. Cells 40 (1996) 123.
[7] T.E. Varitimos, R.W. Tustison, Thin Solid Films 151 (1987) 27.
[8] P.P. Hankare, P.A. Chate, D.J. Sathe, J. Alloys Compd. 487 (2009) 367.
[9] P.P. Hankare, P.A. Chate, D.J. Sathe, B.V. Jadhav, J. Alloys Compd. 490 (2010) 350.
[10] J. Cheng, D. Fan, H. Wang, B. Liu, Y. Zhang, H. Yan, Semicond. Sci. Technol 18 (2003) 676.
[11] N. Fathy, M. Ichimura, Sol. Energy Mater. Sol. Cells 87 (2005) 747.
[12] N. Fathy, R. Kobayashi, M. Ichimura, Mater. Sci. Eng. B 107 (2004) 271.
[13] C. Cruz-Vazquez, F. Rocha-Alonzo, S. Burruel-Ibarra, M. Barboza-Flores, R. Bernal, M. Inoue, Appl. Phys. A 79 (2004) 1941.
[14] V. Kumar, M. Sharma, J. Gaur, T. Sharma, Chalcogenide Lett. 5 (2008) 289.
[15] M. Oztas, M. Bedir, S. Ocak, R. Yldurum, J. Mater. Sci.: Mater. Electron. 18 (2007) 505.
[16] P.P. Hankare, P.A. Chate, S.D. Delekar, M.R. Asabe, I.S. Mulla, Phys. Chem. Solids 67 (2006) 2310.
[17] C.D. Lokhande, P.S. Patil, H. Tributsch, A. Ennaoui, Sol. Energy Mater. Sol. Cells 55 (1998) 379.
[18] A. Schmidt, J. Cryst. Growth 101 (1990) 758.
[19] A. Samantilleke, M. Boyle, J. Young, I. Dharmadasa, J. Mater. Sci.: Mater. Electron. 9 (1998) 231.
[20] H. Luo, T.K. Furdyna, Semicond. Sci. Technol. 10 (1995) 1041.
[21] R.B. Kale, C.D. Lokhande, Mater. Res. Bull. 39 (2004) 1829.
[22] J. Jan, S. Kuo, S. Yin, W. Hsich, Chin. J. Phys. 39 (2001) 90.
[23] Y. Mitusumori, Y. Ohkubo, A. Hasegawa, M. Sasaki, F. Minami, J. Lumin. 108 (2004) 259.
[24] M. Bouroushian, D. Karoussos, T. Kosanovic, Solid State Ionics 177 (2006) 1855.
[25] P.P. Hankare, A.H. Manikshete, D.J. Sathe, P.A. Chate, K.C. Rathod, Mater. Chem. Phys. 113 (2009) 183.
[26] K.L. Chopra, S. Das, Thin Films Solar Cells, Plenum, New York, 1983, p. 229.
[27] C. Estrada, P. Nair, M. Nair, R. Zingaro, E. Meyers, J. Electrochem. Soc. 141 (1994) 802.
[28] B. Mokili, Y. Charreire, R. Cortes, D. Lincot, Thin Solid Films 288 (1996) 21.
[29] J. Dona, J. Herrero, J. Electrochem. Soc. 141 (1994) 205.
[30] D.A. Johnston, M.H. Carletto, K.T.R. Reddy, I. Forbes, R.W. Miles, Thin Solid Films 403 (2002) 102.
[31] M. Bouroushian, Z. Loizos, N. Spyrellis, G. Maurin, Appl. Surf. Sci. 115 (1997) 103.
[32] F. Gode, C. Gumus, M. Zor, J. Cryst. Growth 299 (2007) 136.
[33] S.M. Sze, Physics of Semiconductor Devices, 2nd ed., Wiley, NY, 1969.
[34] F.I. Ezema, A.B. Ekwealor, R.U. Osuji, Turk. J. Phys. 30 (2006) 157.
[35] A. Goudarzi, G. Aval, R. Sahraei, H. Ahmadpoor, Thin Solid Films 516 (2008) 4953.